Spindle-to-cortex communication in cleaving, polyspermic *Xenopus* eggs

Christine M. Field, Aaron C. Groen, Phuong A. Nguyen, and Timothy J. Mitchison
Department of Systems Biology, Harvard Medical School, Boston, MA 02115; Marine Biological Laboratory, Woods Hole, MA 02143

ABSTRACT **Mitotic spindles specify cleavage planes in early embryos by communicating their position and orientation to the cell cortex using microtubule asters that grow out from the spindle poles during anaphase. Chromatin also plays a poorly understood role. Polyspermic fertilization provides a natural experiment in which aster pairs from the same spindle (sister asters) have chromatin between them, whereas asters pairs from different spindles (nonsisters) do not. In frogs, only sister aster pairs induce furrows. We found that only sister asters recruited two conserved furrow-inducing signaling complexes, chromosome passenger complex (CPC) and Centralspindlin, to a plane between them. This explains why only sister pairs induce furrows. We then investigated factors that influenced CPC recruitment to microtubule bundles in intact eggs and a cytokinesis extract system. We found that microtubule stabilization, optimal starting distance between asters, and proximity to chromatin all favored CPC recruitment. We propose a model in which proximity to chromatin biases initial CPC recruitment to microtubule bundles between asters from the same spindle. Next a positive feedback between CPC recruitment and microtubule stabilization promotes lateral growth of a plane of CPC-positive microtubule bundles out to the cortex to position the furrow.**

Monitoring Editor
Rong Li
Johns Hopkins University

Received: Apr 20, 2015
Revised: Aug 17, 2015
Accepted: Aug 18, 2015

INTRODUCTION

Cleavage furrows in early metazoan embryos typically ingress on a plane defined by the metaphase plate of the mitotic spindle. How spatial information encoding the position and orientation of the spindle is transmitted to the cortex to position the furrow is unclear. In eggs, cleavage planes are induced between pairs of microtubule asters that grow out from centrosomes at the two poles of a mitotic spindle, and spindle position is communicated in part by the geometric relationship between these asters. The furrow is induced at the border between the asters at the time they reach the cortex (Rappaport, 2005). In *Xenopus*, where the egg is large (~1.2 mm) compared with the first mitotic spindle (~60 µm), it takes many minutes for microtubule asters to grow out to touch the cortex after anaphase onset, and the distance between the cortex and the centrosomes at the time of furrow initiation is very large on a molecular scale (Mitchison *et al.*, 2012). Thus a spatially robust mechanism is required to transmit information on spindle position and orientation to the cortex.

A classic approach to the problem of how spindles communicate to the cortex has been to ask whether any pair of microtubule asters induce a furrow between them or some special conditions must be met. Polyspermic fertilization in frogs provides a natural experiment in which different types of aster pairs can be generated in a single egg. When polyspermic *Rana* eggs entered anaphase, furrows were induced between pairs of asters that grew out from the same mitotic spindle, which we will call "sister asters." They were *not* induced between pairs of asters that grew out from different spindles, which we will call "nonsister asters" (Brachet, 1910; Herlant, 1911). This classic observation, which was later confirmed in *Xenopus laevis* eggs (Render and Elinson, 1986), is diagrammed in Figure 1. One interpretation of these data is that the presence of chromatin between aster pairs is necessary for them to induce an furrow, which would imply that both chromatin and microtubules are involved in signaling from spindle to cortex to position furrows. Consistent with a positive signal from chromatin to the cortex, cells forced to

This article was published online ahead of print in MBoC in Press (http://www.molbiolcell.org/cgi/doi/10.1091/mbc.E15-04-0233) on August 26, 2015.

Address correspondence to: Christine M. Field (Christine_Field@hms.harvard.edu).

Abbreviations used: AurkA, Aurora kinase A; AurkB, Aurora kinase B; CPC, chromosome passenger complex; GFP, green fluorescent protein; IgG, immunoglobulin G.

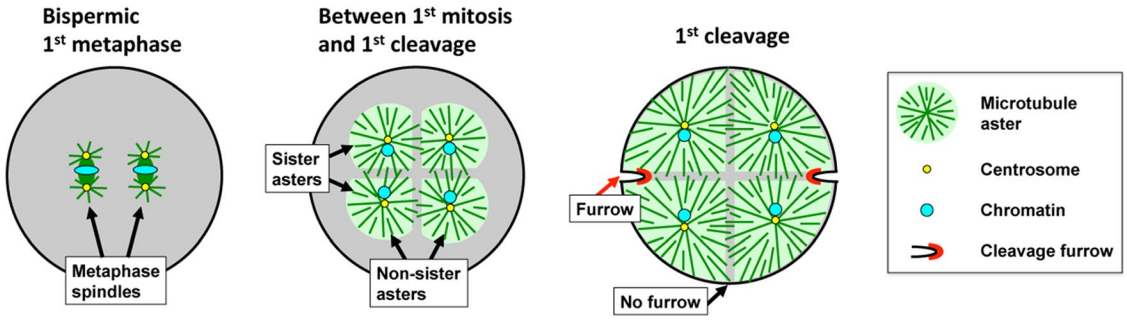

FIGURE 1: Cleavage pattern in a bispermic frog egg. Metaphase spindles in *Xenopus* are ~50–60 µm long in a 1.2-mm egg. After anaphase onset, the small asters at the spindle poles grow steadily until they fill the cell. Asters from the two poles of the same spindle (sister asters) contact each other soon after anaphase onset at the plane previously occupied by the metaphase plate. Asters from the poles of two different spindles (nonsister asters) contact each other later. In both cases, aster growth halts where the asters contact each other, and a zone of lower microtubule density is observed at the aster–aster interaction zone (gray shading). When asters grow to touch the cortex, furrows initiate between sister aster pairs but not between nonsister pairs. Adapted from Brachet (1910), Wühr *et al.* (2009), Snook *et al.* (2011), and Mitchison *et al.* (2012).

undergo monopolar cytokinesis induced cleavage furrows only on the side of the cell nearest to chromatin (Canman *et al.*, 2003; Hu *et al.*, 2008).

A requirement for chromatin for furrow induction is not universal. In a famous experiment using micromanipulated echinoderm eggs, Rappaport showed that furrows were induced between nonsister aster pairs as well as between sisters (Rappaport, 1961, 2005). This experiment proved that aster pairs did not have to grow out from the same spindle to induce a furrow between them, and therefore chromatin was not required for furrow induction. The discrepancy with the polyspermic frog egg observations has not been explained. The Rappaport experiment was reinvestigated in echinoderm eggs using molecular markers (Argiros *et al.*, 2012). Here we reinvestigate cleavage after polyspermic fertilization in the frog *Xenopus laevis*, and in the *Discussion* we compare results between systems.

Cleavage furrow induction depends on two conserved signaling complexes that bind to microtubules—the chromosome passenger complex (CPC; a 1:1:1:1 complex between INCENP, Aurora B kinase [AurkB], Dasra [CDCA8 or 9], and survivin [BIRC5]; Carmena *et al.*, 2012; Kitagawa and Lee, 2015) and Centralspindlin (a 2:2 complex between MKLP1 [Kif23] and RacGap1; White and Glotzer, 2012). In somatic cells, these complexes localize to midzone microtubule bundles after anaphase onset. In *Xenopus* eggs, they localize to a plane that bisects the cell at the location previously occupied by the metaphase plate but extend all the way to the cortex (Nguyen, Groen, *et al.*, 2014). Where one or both of these complexes touch the cortex, they induce cleavage furrows by locally activating the RhoA pathway. The furrow then ingresses along the plane defined by the signaling complexes (Glotzer, 2005; Eggert *et al.*, 2006). Although both CPC and Centralspindlin are implicated in cleavage furrow induction in all animal cells, their relative roles may vary. In a cell-free system derived from *Xenopus* eggs, CPC activity, but not the Kif23 subunit of Centralspindlin, was required for local activation of RhoA on a model plasma membrane (Nguyen, Groen, *et al.*, 2014), suggesting that the CPC plays a more important role in furrow specification in *Xenopus* eggs. Here we focus mainly on the role of the CPC in spindle-to-cortex communication because of its central role in *Xenopus* eggs.

The mechanisms by which the CPC is recruited to microtubule bundles during cytokinesis are complex and poorly understood. The INCENP subunit has direct microtubule- binding sites (Carmena *et al.*, 2012), and two kinesins, Kif4A and Kif20A (MKlp2), are also involved in CPC targeting (Gruneberg *et al.*, 2004; Nunes Bastos *et al.*, 2013; Kitagawa *et al.*, 2014; Nguyen, Groen, *et al.*, 2014). CPC binds to chromatin during metaphase, which led Cooke *et al.* (1987) to propose that it is handed off from chromatin to microtubules at anaphase onset. Consistent with this model, photobleaching showed that the CPC binds dynamically to chromosomes in metaphase but is more static on microtubule bundles during anaphase and cytokinesis (Murata-Hori and Wang, 2002; Delacour-Larose *et al.*, 2004). The CPC generates kinase activity gradients in anaphase, which may promote correct localization (Fuller *et al.*, 2008). Microtubule binding activates the kinase activity of CPC, probably by promoting transphosphorylation of the AurkB and INCENP subunits (Kelley *et al.* 2007**).** Once activated, AurkB kinase activity is believed to promote microtubule polymerization and stabilization. Several mechanisms may be involved, including CPC regulation of Kif4A (Nunes Bastos *et al.*, 2013), KifC1 (MCAK; Ohi *et al.*, 2004), stathmin (Kelly *et al.*, 2007), and EB1 family members (Zimniak *et al.*, 2009; Ferreira *et al.*, 2013) Positive feedback between AurkB activity and microtubule stabilization has been proposed during assembly of cytokinesis midzones in somatic cells (Hu *et al.*, 2008; Nunes Bastos *et al.*, 2013) and meiosis II spindles in eggs (Tseng *et al.*, 2010).

Here we reinvestigated the origin of the cleavage pattern in polyspermic frog eggs by imaging CPC and Centralspindlin in addition to microtubules. Our data partly solve a classic puzzle in fertilization biology and suggest a mechanism by which information on spindle position is transmitted from the spindle at the center of the egg to the cortex to position the cleavage furrow.

RESULTS

One furrow forms per sperm in polyspermic *Xenopus* eggs

We induced polyspermic fertilization of *Xenopus laevis* eggs using sodium iodide treatment and followed eggs by time-lapse microscopy. As previously reported (Render and Elinson, 1986), polyspermic eggs were identified in time-lapse movies by concentration of cortical pigment into patches over centrosomes and nuclei starting ~50 min after fertilization, late in the interphase before first mitosis. When cleavage initiated, each dark patch was cleaved by a single furrow (Supplemental Figure S1). These observations confirm that only one furrow is induced per sperm when one to four sperm enter the egg, and the furrow only cleaves between sister aster pairs, as diagrammed for a bispermic egg in Figure 1. Highly polyspermic eggs formed many furrows that fused and regressed unpredictably, making them difficult to analyze.

Visualization of aster pairs in fixed monospermic eggs

To investigate the normal situation, we fixed monospermic eggs after first mitosis and before or during first cleavage and stained for microtubules and cytokinesis signaling complexes using fluorescently labeled antibodies anti-AurkB for CPC and anti-Kif23 to image Centralspindlin. Figure 2A shows an egg fixed soon before cleavage onset. The sister asters are dome shaped, and a planar interaction zone of lower microtubule density forms where they meet at midcell. CPC was dramatically enriched at this interaction zone. Centralspindlin was also enriched at the interaction zone, although the staining was dimmer and the enrichment less dramatic. Kif23 staining was always fainter than CPC probing with anti-AurkB or anti-INCENP (unpublished data). This was observed probing with two independent antibodies to Kif23 (unpublished data). This intensity difference possibly reflects the lower concentration in eggs of Kif23 (~20 nM) compared with the CPC (~150 nM; Wühr *et al.*, 2014).

Localization of cytokinesis signaling complexes in polyspermic eggs

In polyspermic eggs fixed in late anaphase of first mitosis, we observed well-separated anaphase spindles that were indistinguishable from those seen in monospermic eggs. Figure 2B shows a bispermic example. At this stage, the asters had grown sufficiently that sister pairs had contacted each other at the center of each anaphase spindle but not yet sufficiently for nonsister asters to contact each other. AurkB localized strongly to microtubule bundles on a plane bisecting each spindle and extended outward to an extent that depended on aster radius. Kif23 was only faintly localized at this stage, indicated by the blue arrow in Figure 2B.

In polyspermic eggs fixed later in the interval between first mitosis and first cleavage, we observed interactions between both sister and nonsister aster pairs (tubulin staining in Figure 2, C and D). A distinct zone of reduced microtubule density was evident for both types of aster–aster interaction. In most cases, the zone of lower microtubule density at the boundary between the asters was more distinct for zones formed between sister asters (see tubulin in Figure 2, C and D). We used microtubule morphology to determine which asters pairs were sisters versus nonsisters. A pair of opposed microtubule tufts with increased density compared with the rest of the aster, resembling a cytokinesis midzone in somatic cells, connected sister aster pairs at the position previously occupied by the spindle. An example of these tufts is seen connecting the upper left aster pair in Figure 2C. On the basis of this criterion, we indicate sister pairs in Figure 2 using double-headed blue arrows. Note that the midzone-like tuft of microtubules connecting sister asters was only present in a few focal planes in a confocal stack and may not be evident in the image planes shown. Midzone-like microtubules tufts were no longer visible in eggs where cleavage had initiated, but in those eggs, we could often infer which asters were sisters by the location of nuclei, which stained with AurkB at this stage, as in Figure 2A.

In eggs fertilized with two to four sperm, we reproducibly observed CPC and Centralspindlin localizing to microtubule interaction zones formed between sister asters but not to zones formed between nonsister asters (Figure 2, C and D). This observation was highly reproducible for eggs fertilized with two to four sperm; we observed no exceptions to this rule in >40 examples of polyspermic eggs. The difference was essentially binary; the CPC staining intensity was strongly elevated over the local background value in zones between sister asters and was approximately the same as the local background in the zone between nonsister asters. We also investigated localization of another conserved cytokinesis midzone protein, Kif4A, in polyspermic eggs. This kinesin has been implicated in blocking growth of midzone microtubule plus ends and also in targeting the CPC (Bieling *et al.*, 2010; Hu *et al.*, 2011; Nguyen, Groen, *et al.*, 2014). We observed enrichment of Kif4A on microtubule bundles in the interaction plane between sister asters but not between nonsister asters (Supplemental Figure S2). Thus Kif4A is recruited in a manner similar to CPC and Centralspindlin, implying that microtubule bundles between sister asters resemble somatic cell midzones in their biochemistry, whereas bundles between nonsister asters do not.

Kinase activity of the AurkB subunit of the CPC is required for furrow induction in *Xenopus* (Nguyen, Groen, *et al.*, 2014), and both CPC and Centralspindlin are required for furrowing in many systems (Glotzer, 2005; Eggert *et al.*, 2006). Thus the difference in recruitment of CPC and Centralspindlin presumably explains why sister aster pairs induce furrows between them and nonsister aster pairs do not (Figure 1). This observation immediately raises the question of what controls differential recruitment of cytokinesis signaling complexes to interactions zones formed between sister versus nonsister aster pairs.

CPC recruitment between nonsister asters in highly polyspermic eggs

The rule that only sister aster pairs recruited CPC between them was broken in highly polyspermic eggs (Figure 2E). In these cases, we observed CPC-positive interaction zones between asters that were clearly nonsisters (yellow arrows in Figure 2E). In these eggs, all asters start close together and close to chromatin, due to the general crowding of the egg. We speculate that one or both of these conditions explain why nonsister aster pairs recruited CPC between them in highly polyspermic eggs, although they did not in eggs containing two to four sperm.

Forced activation of the CPC increased furrowing in monospermic eggs

To test for a causal relationship between CPC recruitment and furrowing in eggs, we used a gain-of-function approach. We made an activating antibody (immunoglobulin G [IgG]) against INCENP, copying a design of Kelly *et al.* (2007) that was shown to activate AurkB kinase activity by cross-linking the CPC. We injected CPC-activating IgG into fertilized frog eggs. To focus on cleavage and avoid perturbation of first mitosis, we performed all injections 60–70 min after fertilization, a time when first mitosis was complete but first cleavage had not yet initiated. This is the time window in which the aster pairs are growing toward the cortex to initiate cleavage.

When this CPC-activating antibody was injected into monospermic eggs, we observed formation of multiple ectopic furrows at the time of normal cleavage (Figure 3A). In injected eggs fixed during first cleavage, we observed ectopic recruitment of the CPC to microtubule arrays (Figure 3B). Where planes of CPC-positive microtubules met the cortex, they induced ectopic furrows (Figure 3B, white arrows). CPC-activating IgG did not cause uniform recruitment of the CPC to microtubules. The CPC was always enriched at the peripheries of microtubule arrays, whether or not these were participating in aster–aster interactions, and it tended to form planes, which were visualized as lines in optical sections (Figure 3B). See Supplemental Tables S1 and S2 for quantitation.

Microtubule dependence of furrowing

Nocodazole (50 μM) completely blocked furrowing of normally fertilized eggs by time lapse, as expected (Rappaport 2005). It also

completely blocked ectopic furrowing in fertilized eggs injected with activating anti-INCENP IgG (Supplemental Figure S3 and Supplemental Table S1). Thus microtubules are required for ectopic furrowing induced by CPC activation.

Microtubule stabilization increased CPC recruitment and furrowing in eggs

In *Xenopus* extracts, the CPC can be activated by binding to microtubules (Tseng *et al.*, 2010). To test whether increasing microtubule stability (and density) increased furrowing, we injected monospermic eggs with inhibitory IgG to the catastrophe factor MCAK (Kif2C), which is a potent microtubule-destabilizing factor in frog eggs (Walczak *et al.*, 1996). Injections were carried on the same time frame as before (injection at 60–70 min postfertilization but before first cleavage). By time lapse, we noted multiple ectopic furrows, similar to anti-INCENP injections (Figure 3C). In anti-MCAK–injected eggs fixed before or during furrowing, we noted increased microtubule density and induction of extra asters, as expected from previous observations inhibiting MCAK in egg extract (Walczak *et al.*, 1996). These enhanced asters strongly recruited CPC to their expanding peripheries, even where there was no evidence of antiparallel overlap (Figure 3D; see Supplemental Tables S1 and S2 for quantitation). Thus, increasing microtubule density and/or stability promoted ectopic recruitment of the CPC to aster peripheries and, subsequently, induction of ectopic furrows. Buffer injection had no effect on cleavage (Figure 3, E and F, and Supplemental Tables S1 and S2).

To nucleate and stabilize microtubules by a different mechanism, we microinjected Taxol. We observed assembly of ectopic, highly bundled microtubule arrays that strongly recruited CPC to one edge, usually in a single location presumably corresponding to the injection site (Supplemental Figure S4). Thus, stabilizing microtubules with Taxol also forces CPC recruitment in eggs. We did not observe ectopic furrowing and suspect that this is because the microinjected Taxol and the microtubules it induced tended to remain localized near the center of the egg. For this reason, Taxol-induced, CPC-positive microtubules do not touch the cortex and thus cannot induce ectopic furrows.

Forced recruitment of CPC to zones between nonsister asters

We next asked whether we could force CPC recruitment at interaction zones formed between nonsister asters, which are normally CPC-negative (Figure 2, C and D). We injected the activating anti-INCENP IgG into polyspermic eggs and fixed them before first cleavage. In anti-INCENP–injected eggs fertilized with two sperm, we observed that CPC recruitment to zones formed between sister and nonsister aster pairs with similar intensity (Figure 4, A and B). An image of uninjected bispermic egg fixed at a similar stage is included for comparison (Figure 4C). This experiment was technically challenging because we could not control the degree of polyspermy, and we recovered only a few bispermic examples. Three of four injected, bispermic eggs exhibited an additional, CPC-positive interaction zone between nonsister asters. Thus artificial activation of the CPC forces its recruitment to interaction zones between nonsister asters, which are normally CPC negative. Analysis of cleavage pattern in anti-INCENP–injected polyspermic eggs with more than two sperm was complicated. When we could clearly distinguish sister versus nonsister aster pairs, we found that seven of eight eggs fertilized with three to six sperm exhibited one or more AurkB-positive nonsister interaction zones (unpublished data).

Effects of CPC activation and microtubule stabilization in egg extract

To gain mechanistic insights into the interrelationship between CPC activation and microtubule stabilization seen in eggs, we turned to a recently reported *Xenopus* egg extract cytokinesis system. This system reconstitutes both recruitment of CPC to microtubule bundles between asters and also downstream cytokinesis signaling events when placed on artificial lipid bilayers (Nguyen, Groen, *et al.*, 2014). CPC was imaged using directly labeled AurkB antibody (Figures 5 and 6) or green fluorescent protein (GFP)–DasraA (Figure 7) with similar results. Asters were nucleated from beads coated with an activating antibody to Aurora kinase A (AurkA; Tsai and Zheng, 2005), which avoids complications from chromatin (see later discussion). Large asters grew out from the beads, and where they met, CPC-positive interaction zones formed (Figure 5A, control, and Supplemental Movie S5A Control). This result is as previously reported (Nguyen, Groen, *et al.*, 2014). Here we analyzed many fields at low magnification and noted that only a subset of aster–aster interactions recruited CPC. We tested whether the molecular perturbations that induced ectopic furrows in eggs, INCENP activation and MCAK inhibition, as well as Taxol, also increased formation of CPC-positive zones in extract. By eye, formation of CPC-positive aster–aster interaction zones was enhanced by activating the CPC or stabilizing microtubules, as evidenced by more CPC-positive zones per field and in some cases earlier formation of those zones (Figure 5, A and B). In some sequences, the CPC-positive state appeared to spread laterally from the initial point of microtubule interaction, suggesting the possibility of nucleated assembly (Supplemental Movies S5A Control and S5B Taxol). To quantify CPC recruitment, we made movies of multiple fields at 10× and quantified the total length of CPC-positive zones per field divided by the number of nucleating beads in that field. Normalization to bead density corrects for greater potential zone length in fields containing more beads. These data confirmed that forced CPC activation or microtubule stabilization by two means stimulated formation of CPC-positive interaction zones between asters (Figure 5C). Thus CPC recruitment to aster microtubules is regulated in a similar manner in both intact eggs and egg extracts. In both cases, CPC recruitment is stimulated by both CPC activation and microtubule stabilization.

Starting distance between asters influences CPC recruitment

Not all interaction zones between AurkA bead asters recruited CPC in control extract (Figure 5A). By analyzing pairwise interactions between beads, we determined that the initial distance between beads correlated with whether they did or did not generate a CPC-positive zone between them. Bead pairs that started very close (yellow arrowheads in Figure 6A) or very far apart (blue arrowheads) usually failed to induce a CPC-positive zone between them upon aster–aster contact. Zones that were initially CPC-negative but then recruited CPC via a lateral spreading mechanism from neighboring CPC zones were scored as CPC-negative. Using this strategy, we counted 15 of 24 CPC-positive zones and nine of 24 CPC-negative zones in a representative experiment shown in Figure 6A. Figure 6B shows a histogram in which image sequences were collected from multiple positions using an automated stage. The *x*-axis is the initial bead-to-bead distance, and separate histograms are plotted for bead pairs that did or did not recruit CPC to a zone between them by the end of the movie. Note that CPC recruitment tended to fail at very short and very long initial distances. Initial separation distance is obligatorily coupled to the time when asters meet in this

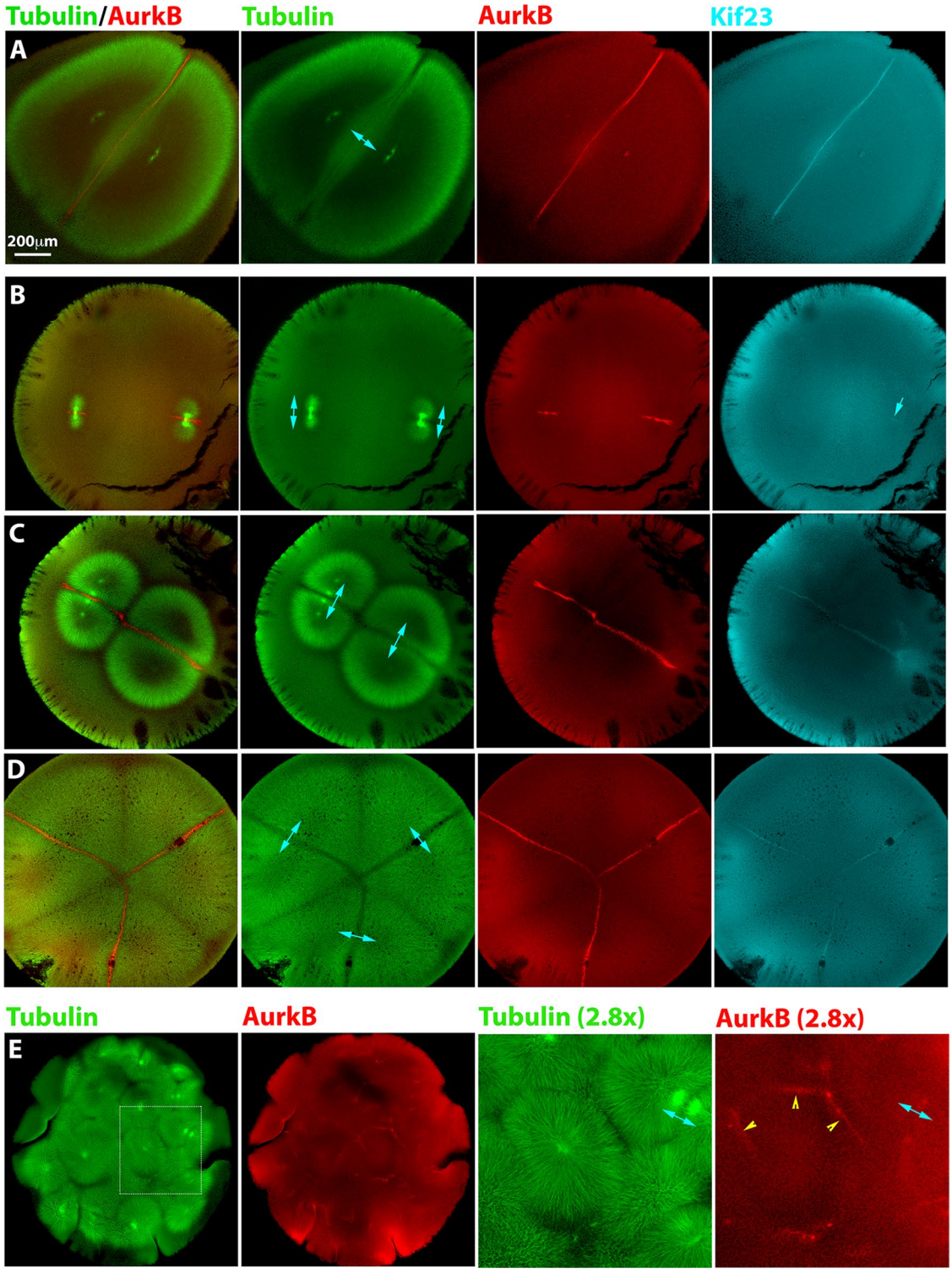

FIGURE 2: Localization of furrow-inducing protein complexes in polyspermic eggs. Eggs were fixed between first mitosis and first cleavage, stained for AurkB (a subunit of the CPC) and Kif23 (a subunit of Centralspindlin), and imaged by confocal microscopy. Cyan double-headed arrows illustrate sister aster pairs. (A) Normal, monospermic egg. Note plane of CPC- and Centralspindlin-positive microtubule bundles between sister asters. (B) Bispermic egg fixed a few minutes after anaphase onset. The asters have just started to grow. A CPC-positive disk is evident at the plane previously occupied by the metaphase plate, where sister asters recently met. Centralspindlin recruitment is less evident (cyan single arrow in Kif23 image). (C) Bispermic egg fixed midway between anaphase and cleavage. Interaction zones between sister and nonsister asters were evident in the tubulin image. Note a brighter tuft of microtubules that connects the sister pair to the upper left, in register with the centrosomes. This midzone-like morphological marker reveals the previous position of the spindle and was used to identify sister aster pairs in microtubule images. CPC and

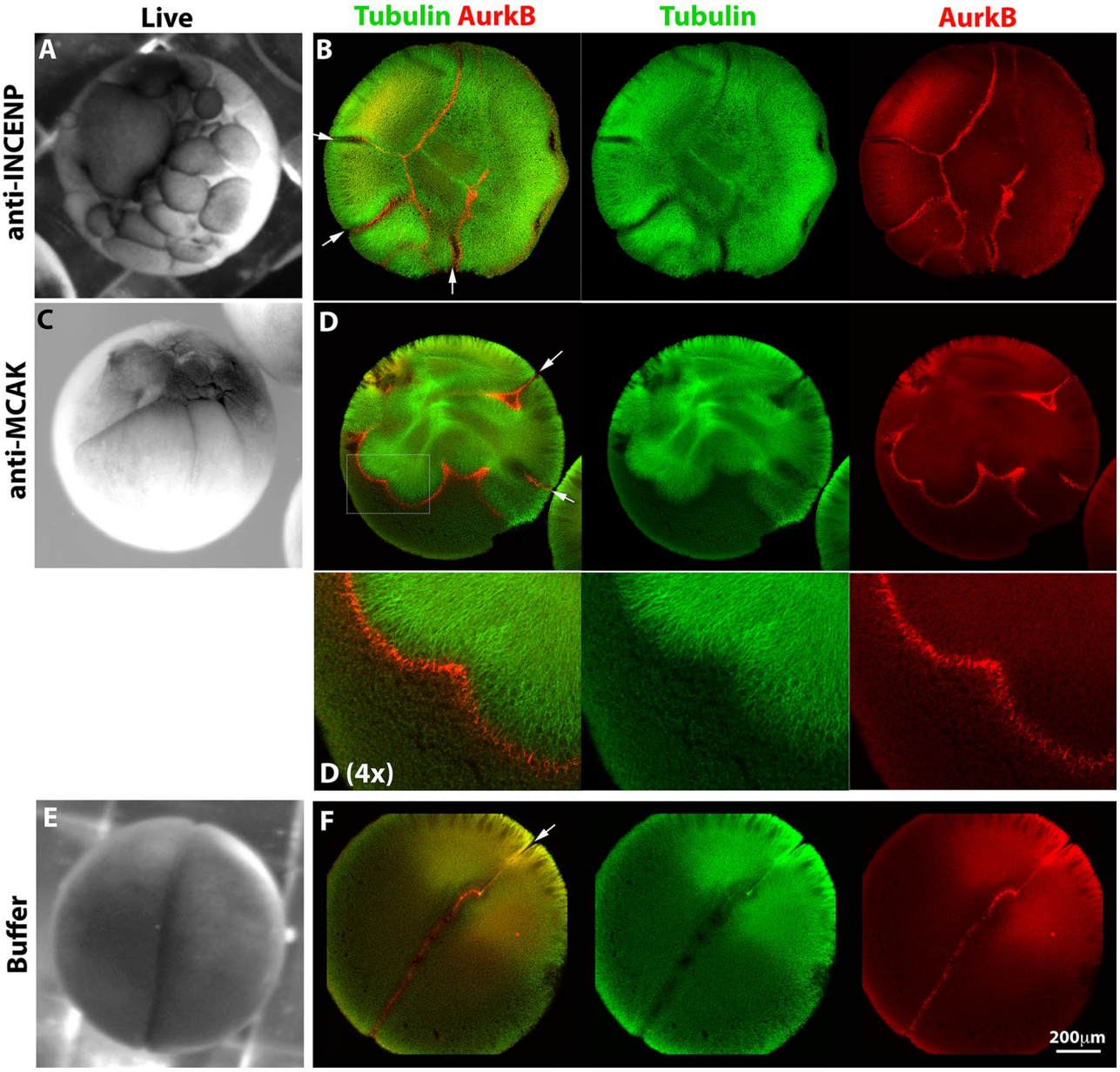

FIGURE 3: Forced activation of the CPC induces ectopic furrows. Monospermic eggs were injected after first mitosis (60–70 min postfertilization) and time-lapse imaged to score cleavage (A, C, E), or fixed around the time of first cleavage and stained for tubulin and AurkB for CPC (B, D, F). (A, B) Injection with an activating anti-INCENP IgG. (A) Note multiple ectopic furrows. (B) Note ectopic microtubule assemblies with CPC strongly localized to their peripheries. Furrows initiated where CPC planes touched the cortex (white arrows). (C, D) Injection with inhibitory IgG to MCAK (Kif2C), the predominant microtubule catastrophe factor in frog eggs. (C) Note multiple ectopic furrows. (D) Note ectopic, CPC-positive microtubule assemblies and associated ectopic furrows (white arrows) as in B. (E, F) Injection with buffer only. A single cleavage furrow forms (E and white arrow in F).

Centralspindlin have been recruited to the interaction zone between sister asters but not to the zone between nonsister asters. (D) Egg with four sperm fixed early in cleavage. Cleavage has initiated near the animal pole (not shown). This image shows a focal plane near the equator, where three aster pairs are visible. Furrowing had not yet occurred in this focal plane, but asters had grown all the way to the cortex. Note selective recruitment of CPC and Centralspindlin to zones between sister asters. (E) Highly polyspermic egg fixed early in cleavage. The region presented at higher magnification shows a single aster with CPC-positive zones at the junction with several neighboring asters (yellow arrowheads). None of these are zones with its sister aster, which is in a different *z*-plane.

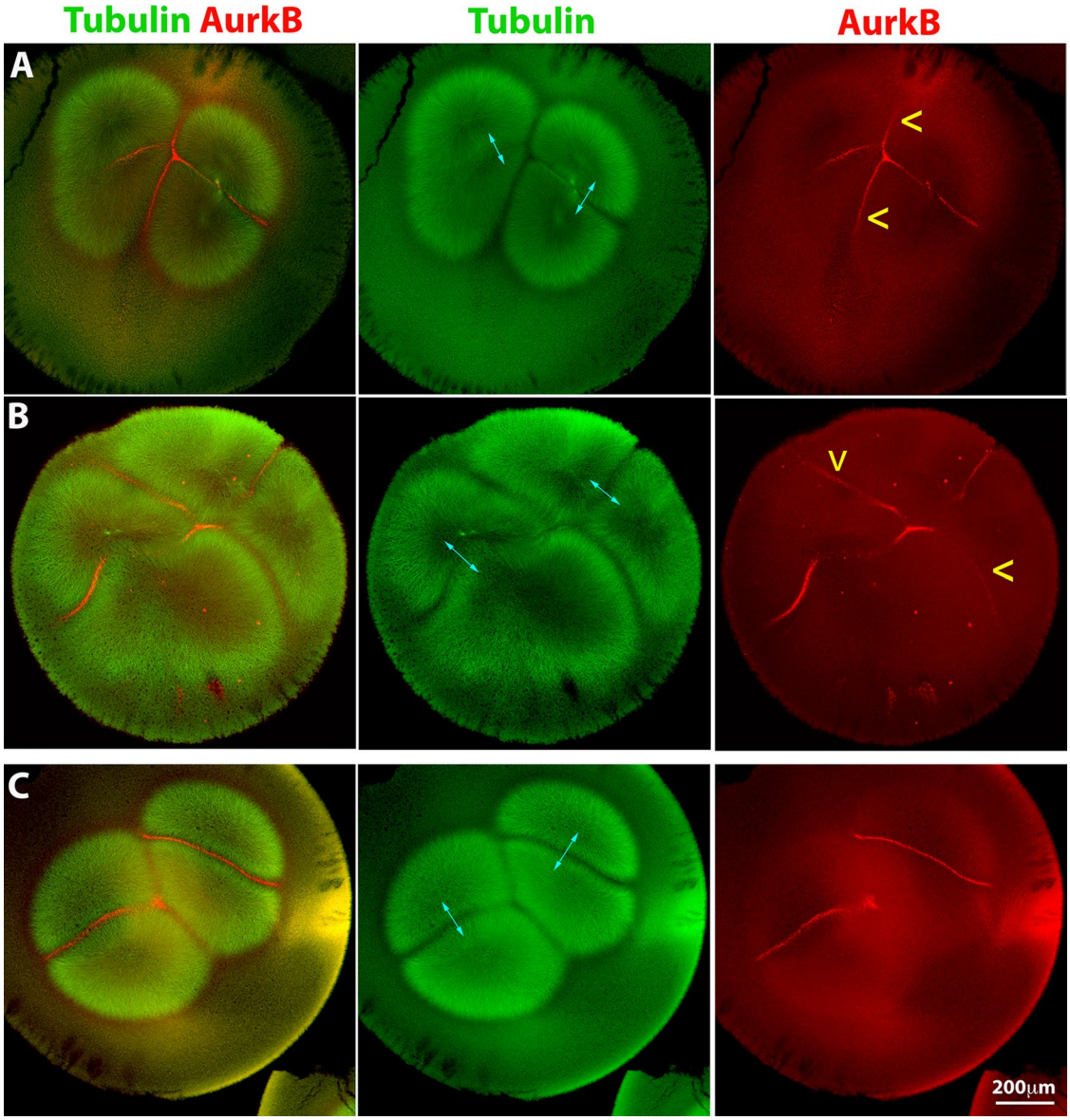

FIGURE 4: Forced activation can recruit the CPC to interaction zones between nonsister asters. An activating anti-INCENP IgG was injected into polyspermic eggs 60–70 min postfertilization (after first mitosis). Sister asters in A–C are indicated by cyan double-headed arrows. (A) Bispermic egg fixed 90 min postfertilization. Note recruitment of CPC at similar levels to the interaction zones between sister and nonsister asters (CPC recruitment between nonsisters is highlighted by yellow arrowheads). Note that the aster morphology has been slightly distorted by the injection. (B) Bispermic egg fixed 98 min postfertilization. Same labeling convention as in A. CPC is recruited to interaction zones between nonsister asters. (C) Uninjected bispermic egg fixed at the same stage as A for comparison. CPC is not recruited between nonsister asters.

experiment. Thus we cannot distinguish whether the preference for an intermediate initial distance is due to an optimal distance or an optimal time after initiating the reaction.

Proximity to chromatin promotes CPC recruitment

Multiple experiments have suggested that chromatin can provide a spatial bias to CPC recruitment to microtubules (see *Introduction*). To test whether proximity to chromatin influences CPC recruitment in *Xenopus* eggs, we modified the extract system by using permeabilized *Xenopus* sperm with attached centrosomes to nucleate asters. The sperm was diluted sufficiently that we could analyze asters that remained isolated, as well as those that interacted with neighbors.

As isolated sperm asters grew, we noted that they usually became polarized, with longer, bushier microtubules on the side furthest from the chromatin and shorter, more-bundled microtubules on the side closest to chromatin (Figure 7, A and A′, and Supplemental Movie S7A). The CPC was recruited preferentially to the aster periphery on the chromatin side, where microtubules were shorter and more bundled (Figure 7, A and A′). Figure 7B shows a field with multiple sperm asters. The seven asters that polarize are labeled p in the DasraA panel, and the one that does not is labeled np. Of the 14 sperm asters in Figure 7, 12 (88%) polarized. A high fraction like this was representative over multiple experiments. See *Materials and Methods* for quantitation.

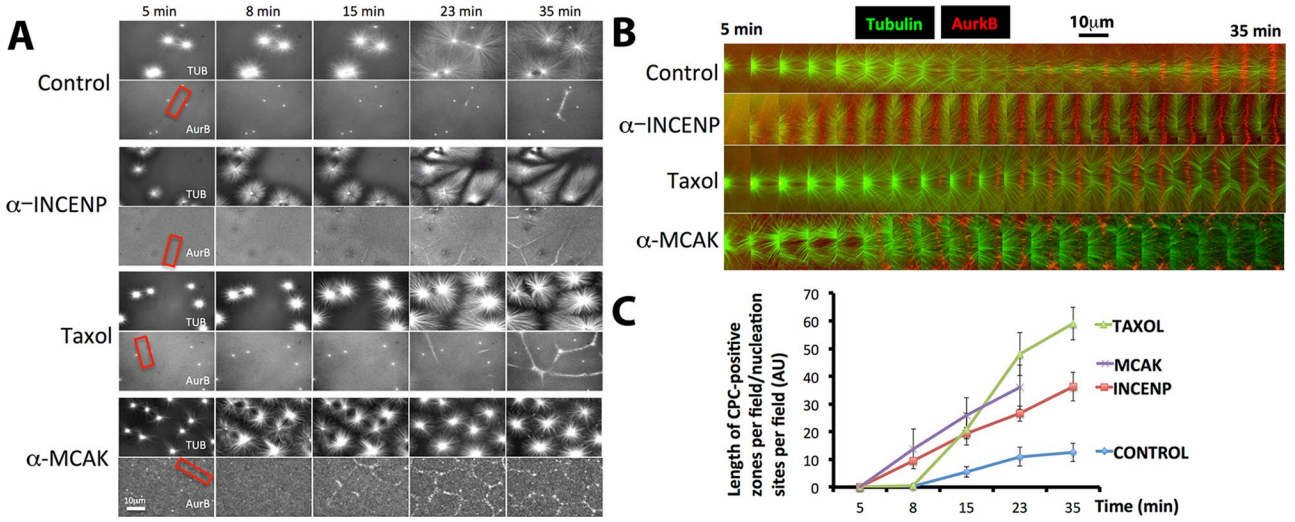

FIGURE 5: Forced activation of the CPC promotes recruitment in the extract system. Interphase egg extracts containing fluorescence probes for tubulin and the CPC (directly labeled anti-AurkB) and beads coated with anti-AurkA as artificial centrosomes. (A) Representative images from time-lapse sequences collected in parallel from the same preparation of extract. Note that more CPC-positive zones were formed between nucleating sites in extracts treated with activating IgG to INCENP, Taxol (0.5 μM final), and inhibitory IgG to MCAK than in control. Once formed, CPC-positive zones were stable for the duration of experiments under all conditions except MCAK inhibition, where they formed early relative to control but then decayed. (B) Higher-magnification image sequences of the regions shown by red boxes in A. Regions were chosen to highlight the establishment and growth of CPC-positive zones between nucleating sites. Note that the zone from control and Taxol-treated extracts grows laterally after it initiates. CPC-positive zones formed earlier when the CPC was activated or microtubules were stabilized. (C) Quantification of CPC-positive zone formation from multiple image fields. At each time point, the length of CPC-positive zones in a field was measured and divided by the number of nucleating beads in the field. Note that CPC stimulation (anti-INCENP), Taxol, and MCAK inhibition all stimulated the rate and extent of CPC-positive zone formation. The last time point was omitted from the MCAK inhibition experiment because CPC-positive zones were unstable under this condition. With regard to A, see Supplemental Movies S5A Control and S5B Taxol.

Sperm asters grew radially on both CPC-positive and -negative sides, although more slowly on the CPC-positive side. The initial angle of the CPC-positive arc varied, and it often spread laterally around the circumference as the aster grew, to the point that the whole aster periphery eventually became CPC-positive in some cases (Figure 7, A–C; also see Supplemental Movies S7A–S7C). When aster pairs grew into contact, they recruited CPC to bundles at the shared boundary, irrespective of the position of chromatin

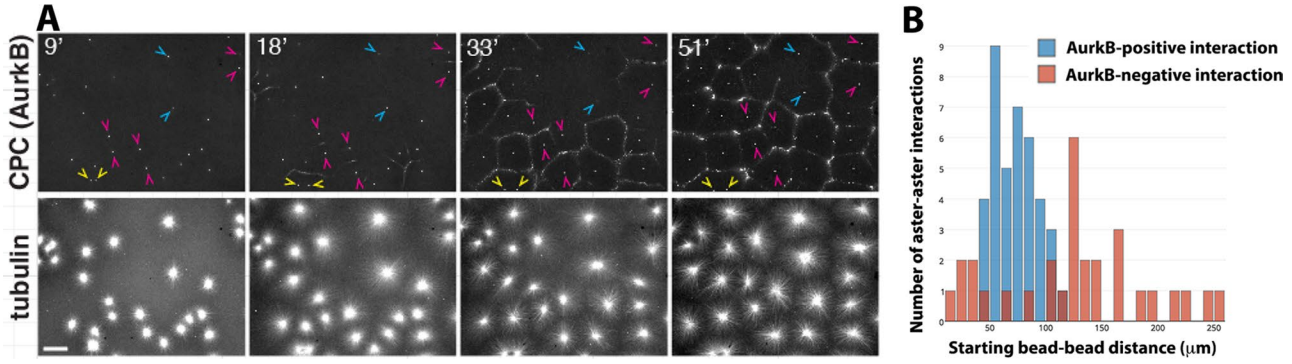

FIGURE 6: Initial distance between nucleating sites influences CPC recruitment. The same experiment as in Figure 5 was performed without molecular perturbations. The CPC probe is directly labeled anti-AurkB, and beads coated with anti-AurkA are the aster nucleators. Bead pairs were identified based on whether their asters interacted at the end of the movie. The distance between the bead pairs was measured at the start of the movie, and whether or not a CPC-positive zone formed between beads was scored upon initial aster–aster contact. (A) Example images from a time-lapse sequence. Arrowheads indicate typical bead pairs. Yellow and blue show examples where AurkB-positive zones did not form between beads; magenta shows examples where AurkB-positive zones did form. Note that the yellow arrowheads are close together ($n = 2$), blue arrowheads are further apart ($n = 7$), and magenta arrowheads are separated by an intermediate distance ($n = 15$). (B). Histogram of initial bead separations plotted separately for bead pairs where an AurkB-positive zone did (blue bars; $n = 39$) or did not (red bars; $n = 30$) form upon aster–aster contact. Initial distances were pooled for multiple fields imaged in parallel in two independent experiments (six fields total). Note that the initial separation distance was unimodal for bead pairs for which a CPC-positive zone did form. The distribution was much more spread out, and possibly bimodal, for bead pairs for which a CPC-positive zone did not form.

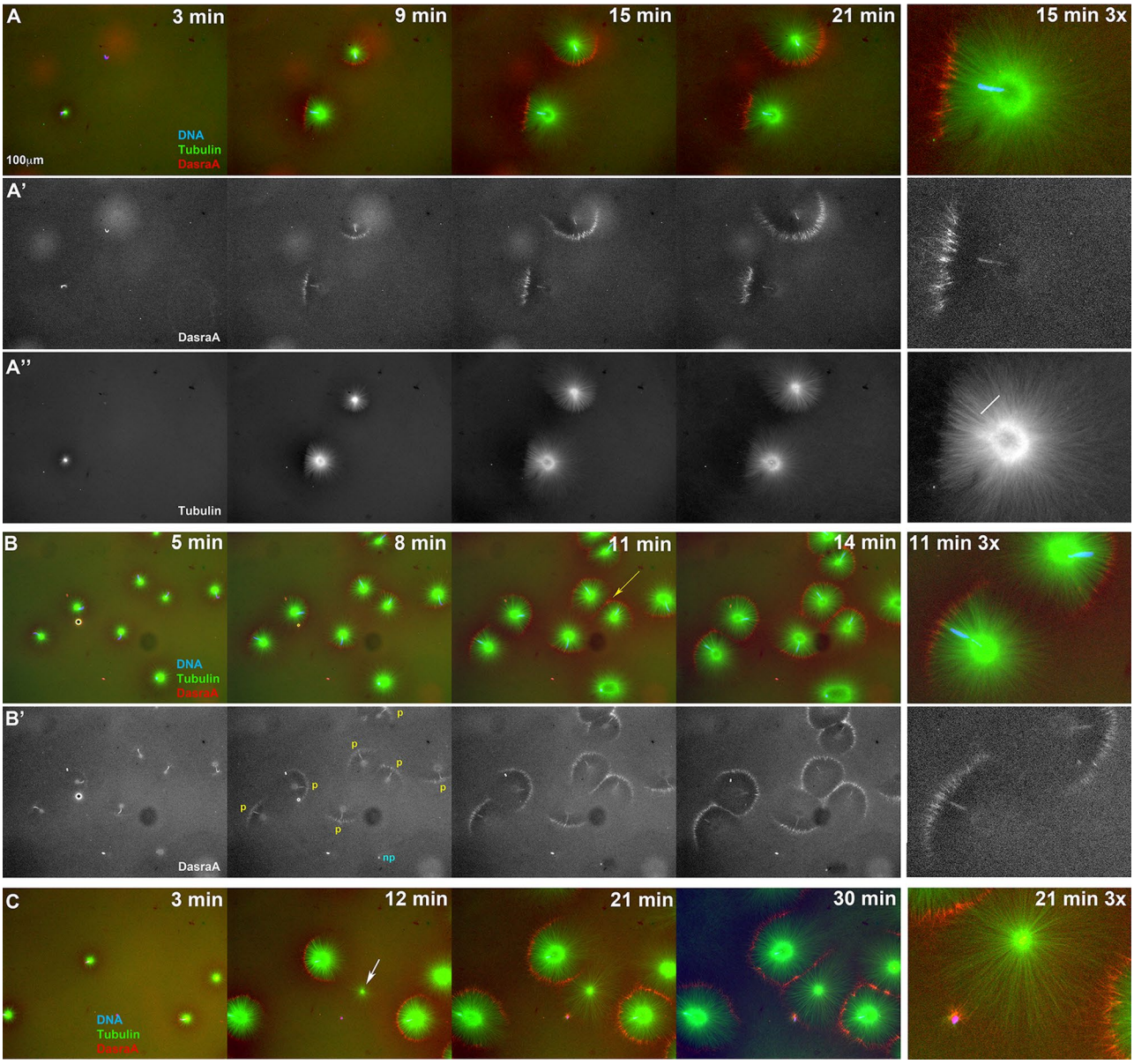

FIGURE 7: Chromatin spatially biases CPC recruitment to monopolar sperm asters in egg extract. Permeabilized sperm was added to interphase egg extract supplemented with probes for DNA, tubulin, and the CPC (GFP-DasraA). (A–C) Image sequences chosen to emphasize different aspects of this reaction. The last in each series is a 3× magnification. Time points are as indicated. (A) Two isolated sperm asters. Note polarized microtubule distribution and formation of an arc of CPC-positive bundles on the periphery of each aster on the same side as the DNA. (A′) Only the DasraA channel for the same images as A. Note that the DasraA probe binds sperm chromatin. (A″) Only the microtubule channel. (B) Field at higher sperm density. (B′) Same images in DasraA channel alone. Seven of eight of the asters polarize early (yellow p), and one aster never polarizes (cyan np). Later most asters contact a neighbor and form a CPC-positive interaction zone; yellow arrow at 11-min time point (B). (C) Field that includes a centrosome not attached to a sperm nucleus (white arrow in 12-min image). The centrosome nucleated a weaker aster than the sperm-attached centrosomes. The free centrosome aster did not recruit CPC to its periphery until it contacted a neighboring aster (30-min time point). The bright dot on the lower left side of the free centrosome aster is DNA without a centrosome. With regard to A–C, see Supplemental Movies 7A–7C, respectively.

(Figure 7, B and C, and Supplemental Movies S7B and S7C). By eye, chromatin and aster–aster interaction zone appeared to contribute approximately equally to CPC recruitment. These experiments showed that both proximity to chromatin and antiparallel overlap can trigger recruitment of the CPC to microtubule bundles. Once recruited, the CPC-positive zone was stable and often spread laterally.

Aster polarization requires DNA and AurkB activity

Our sperm preparations contained free centrosomes (not associated with chromatin). These nucleated asters that were radially symmetric and did not recruit CPC to their periphery unless they interacted with a neighboring aster (white arrow in Figure 7C; see Supplemental Movie S7C). Similar observations were made using beads coated with anti-AurkA to nucleate asters, which were radially

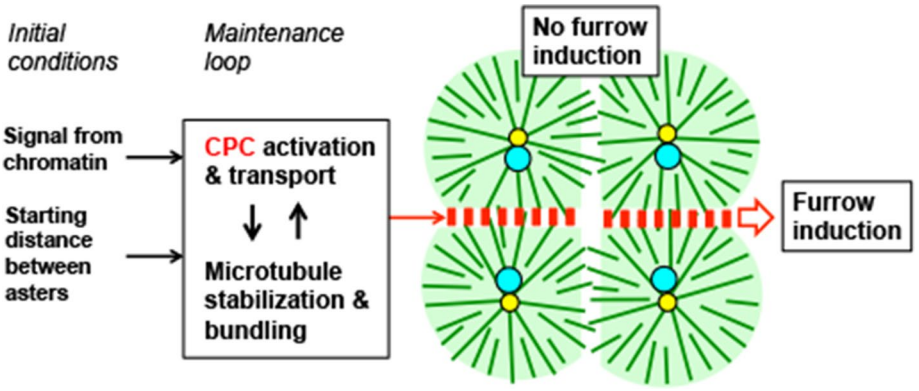

FIGURE 8: Model illustrating results and hypothetical underlying mechanisms. The image illustrates the situation in a bispermic egg between first anaphase and first cleavage, similar to the cartoon in Figure 1 and the experimental examples in Figures 2C and 4C. Color coding and orientation of sister and nonsister aster pairs are as in Figure 1; red boxes indicate CPC and Centralspindlin complexes. The text boxes linked by arrows are factors we identified that control CPC recruitment and activation. We hypothesize that locally acting signals from chromatin (Figure 7) and the starting distance between asters (Figure 6) together provide an initial bias that promotes CPC recruitment between sister asters and are lacking between nonsister asters. We further hypothesize that CPC activation/recruitment (Figures 3–5) and microtubule bundling/stabilization (Figures 3 and 5) together constitute a positive feedback loop that promotes CPC retention on microtubule bundles and lateral spreading of CPC-positive bundles. These positive feedbacks allow a CPC-positive interaction zone to grow radially from the site previously occupied by the metaphase plate all the way to the cortex while retaining its CPC-positive state.

symmetric and did not recruit CPC to their periphery unless they interacted with a nearby aster (Figures 5 and 6; Ishihara *et al.*, 2014; Nguyen, Groen, *et al.*, 2014). Thus chromatin is required for polarized CPC recruitment to asters in the extract system. Addition of the AurkB inhibitor ZM447439 at 40 μM blocked CPC recruitment to the sperm aster periphery in extract and also blocked aster polarization (unpublished data). This is consistent with previous reports that AurkB activity is required for CPC recruitment to microtubule asters in HeLa cells and egg extract (Hu *et al.*, 2008; Nguyen, Groen, *et al.*, 2014). Collectively our data suggest that chromatin locally activates AurkB kinase activity, leading to its localization to the periphery of asters proximal to chromatin.

DISCUSSION

Figure 8 summarizes our results along with a mechanistic interpretation. We illustrate the arrangement of asters in a bispermic egg midway between first anaphase and cleavage, as per Figure 1. It has long been known that in frog eggs, sister aster pairs, which are identified by the chromatin position, induce furrows between them when they reach the cortex, whereas nonsister aster pairs do not (Brachet, 1910; Herlant, 1911). We showed that this is because the cytokinesis- signaling complexes CPC and Centralspindlin are recruited to the interaction zones that form between sister asters and not to the zones between nonsisters (Figure 2). We then explored the factors that determine this difference. Using a combination of whole-egg and extract experiments, we identified three positive influences on CPC recruitment: proximity to chromatin (Figure 7), microtubule stabilization (Figures 3 and 5), and optimal starting distance between asters (Figure 6). Our observations add several new findings to the literature on furrow induction by microtubule in large egg systems. We previously reported the morphology of aster–aster overlap zones (Mitchison *et al.*, 2012) and of the disk of CPC- and Centralspindlin-positive microtubule bundles that grows to the cortex (Nguyen, Groen, *et al.*, 2104). Here we reinforce the importance of the CPC-positive disk as a positive signal that induces furrows by showing that morphologically similar aster–aster overlap zones lacking CPC-positive bundles do not induce furrows. The opposite result was found in echinoderm eggs (Argiros *et al.*, 2012), and we discuss this difference later. Midzone microtubules were previously shown to be stabilized (Canman *et al.* 2003; Foe and von Dassow, 2008). Here we show, for the first time, that artificial stabilization of microtubules by inhibition of a catastrophe factor or addition of Taxol promotes formation of CPC-positive bundles. We also report the first cell-free system for analyzing the positive influence of chromatin on CPC recruitment to anaphase microtubules.

In Figure 8, we propose a conceptual separation between *initial conditions* that positively influence CPC recruitment to an aster–aster interaction zone (proximity to DNA and starting distance) and a *core feedback loop*, based on microtubule stabilization and CPC recruitment, which maintains the CPC-positive state once it has initiated and promotes its lateral growth toward the cortex. As cited in the *Introduction*, positive feedback in CPC recruitment has been proposed before, and multiple mechanisms may be involved, including spatial gradients of kinase activity, kinesin-mediated transport, microtubule bundling, and microtubule stabilization. Here we showed that forced activation of the CPC stimulated assembly of ectopic microtubule arrays (Figure 3) and that forced microtubule stabilization promoted CPC recruitment (Figures 3–5), consistent with positive feedback. Nonsister aster pairs, which never meet the initial conditions, never become CPC-positive at their shared boundary, do not initiate the feedback loop, and therefore do not induce furrows. By separating initial conditions from the feedback loop in Figure 8, we seek to explain how a transient influence from chromatin (and from starting distance) can give rise to a long-lived, CPC-positive disk that grows out to reach the cortex. Our model does not precisely account for how the CPC-positive zone spreads outward as the sister asters grow. Spreading does not require antiparallel microtubules, since we also observed circumferential spreading of CPC-positive bundles at the periphery of growing sperm asters in extract, which are presumably unipolar (Figure 7). Spreading might involve spatial gradients of AurkB kinase activity, bending fluctuations of microtubules, direct physical interactions between CPC complexes on neighboring microtubules, and perhaps CPC transport on a subset of microtubules oriented in the cleavage plane. By initiating at the site previously occupied by the metaphase plate and spreading outward as a plane normal to aster microtubules, the CPC-positive zone transmits information on spindle position and orientation to the cortex to correctly position the furrow. Understanding how this spreading occurs is a key question for future studies.

Rappaport furrows are induced between nonsister aster pairs in some systems but not others. In Table 1, we summarize observations from the four systems for which molecular data have been collected, of which only polyspermic frog eggs do not exhibit Rappaport furrows. The most obvious difference between systems is the much larger spatial scale in frog eggs. This large scale requires a

System	Mammalian tissue culture	*C. elegans* egg	Echinoderm egg	*Xenopus* egg
Cell diameter (μm)	~15	~30	~100	~1200
Rappaport furrows?[a]	Yes	Yes	Yes	No[b]
Microtubule organization in asters	Single microtubules grow from centrosome to cortex	Single microtubules grow from centrosome to cortex	Not known	Most microtubules are nucleated away from centrosome
Equatorial microtubule morphology in cytokinesis	Midzone bundles and aster plus ends at cortex	Midzone bundles and aster plus ends at cortex	Midzone bundles and aster plus ends at cortex	Uniform disk of antiparallel bundles
CPC localization in normal furrows	Midzone, cortex, midbody	Midzone, midbody	Midzone, midbody	Uniform disk
CPC localization in Rappaport furrows	Midbody[c]	Not tested	Not localized (but required)[d]	No Rappaport furrows
Centralspindlin localization in normal furrows	Midzone, cortex, midbody	Midzone, cortex, midbody	Midzone, cortex, midbody	Uniform disk
Centralspindlin localization in Rappaport furrows	Midbody[c]	Not tested	Midzone, cortex, midbody	Not tested

References: mammalian, Reider *et al.* (1997) and Savoian *et al.* (1999); *C. elegans*, Baruni *et al.* (2008), Lewellyn *et al.* (2011), and Basant *et al.* (2015); echinoderm, Rappaport (1961, 2005) and Argiros *et al.* (2012); *Xenopus*, Render and Elinson (1986), Ishihara *et al.* (2014), Nguyen, Groen *et al.* (2014), and this study.
[a]We define a "Rappaport furrow" as a furrow induced between two asters that did not emanate from the poles of the same mitotic spindle, termed "nonsister asters" in this article.
[b]Rappaport furrows were not observed after fertilization with two to four sperm per egg. CPC localization between nonsister asters, presumably followed by Rappaport furrows, could be observed after highly polyspermic fertilization (Figure 2).
[c]Localization of CPC and Centralspindlin in Rappaport furrows in tissue culture cells was only assessed late in cytokinesis in midbodies.
[d]AurkB activity was required for ingression of Rappaport furrows in echinoderm zygotes even though the CPC was not localized between nonsister asters.

TABLE 1: Comparison of Rappaport furrow formation in metazoan systems.

special mechanism for nucleating astral microtubules away from centrosomes (Ishihara *et al.*, 2014) and also a special equatorial microtubule morphology in which a near-uniform plane of CPC- and Centralspindlin-positive microtubule bundles spans the egg (Figure 2). When the spatial scale was decreased in *Xenopus* through highly polyspermic fertilization, and so the distance between centrosomes became comparable to that for normal echinoderm eggs, we observed recruitment of CPC to bundles between nonsister asters (Figure 2E). This was presumably followed by formation of Rappaport furrows. We observed failure of CPC recruitment if asters centers were more than ~120 μm apart, using artificial centrosomes in extract (Figure 6). Rappaport (1969) noted in echinoderms that the tendency of a nonsister aster pair to induce furrows decreased as the distance between them increased, with a maximal distance for furrow induction of ~35 μm. We do not understand the molecular basis of this conserved distance dependence for furrow induction by nonsister aster pairs, and we note that distance and time are related in the problem. The maximum distance between asters for furrow induction might be due to a maximal time delay between anaphase onset and asters meeting to recruit signaling complexes.

Another difference between systems may be in the relative roles of the CPC and Centralspindlin. Basant *et al.* (2015) proposed a linear pathway in which AurkB activates Centralspindlin, and then Centralspindlin alone induces the furrow. Lewellyn *et al.* (2011) argued for a parallel pathway, by which both complexes signal to the cortex independently in *Caenorhabditis elegans*. Argiros *et al.* (2012) argued that ingression of Rappaport furrows depended on AurkB activity, even though the CPC did not localize between nonsister asters. In *Xenopus*, we find a strong correlation between CPC and Centralspindlin localization in both eggs and extracts (Figure 2; Nguyen, Groen, *et al.*, 2014). When we examined their interdependence in extract, we found that AurkB activity was required to localize both, but depletion of the Kif23 subunit of Centralspindlin had no effect on CPC localization, and signaling to RhoA still occurred (Nguyen, Groen, *et al.*, 2014). The CPC and Centralspindlin evidently lie at the heart of microtubule-to-cortex signaling in all animal cytokinesis. It is unclear whether they function in exactly the same way in all systems or their functions differ, perhaps according to the spatial scale of the system. Possibly consistent with variable functions, *Xenopus* oocytes and eggs express unique maternal versions of the borealin (Kelly *et al.*, 2007) and survivin (Tsuchiya *et al.*, 2005) subunits of the CPC and of the CPC-localizing kinesin Kif20A (Nguyen, Groen, *et al.*, 2014). Perhaps these special maternal isoforms are adapted in some way for cleavage of a very large cytoplasm.

MATERIALS AND METHODS

Chemicals

All chemicals were purchased from Sigma-Aldrich, St. Louis, MO, unless otherwise stated.

Whole-egg fertilization, injection, and staining for imaging

Xenopus eggs were collected, fertilized, dejellied, and injected using standard methods (Sive *et al.*, 2000; wiki.xenbase.org/xenwiki/index.php/Protocols). Polyspermic fertilization was induced with sodium iodide using a modification of a reported procedure (Render and Elinson, 1986). Eggs were extruded into MMR (100 mM NaCl, 2 mM KCl, 1 mM $MgCl_2$, 2 mM $CaCl_2$, 0.1 mM EDTA, and 10 mM 4-(2-hydroxyethyl)-1-piperazineethanesulfonic acid [HEPES]–KOH, pH 7.8), quickly rinsed with a small volume of 20 mM NaI in 0.1× MMR, and then partially drained. One-third of a testis per 5-cm dish of eggs was homogenized in 0.75 ml of 1× MMR and added to the eggs. After 90 s to allow sperm attachment, the dish was flooded with 20 mM NaI in 0.1× MMR. After ~20 min, eggs were

dejellied with 2% cysteine and transferred to 0.1× MMR for imaging and fixation.

For injections, eggs were placed in Petri dishes, with mesh attached to the bottom, containing 5% Ficoll 400 in 0.1× MMR. Eggs were injected with calibrated needles using an air-pressure microinjector (Narishige International, East Meadow, NY). Needles (~1.2-mm initial diameter) were pulled with a Micropipette Puller (Sutter Instrument, Novato, CA) and calibrated to inject 10 nl of sample. Control buffer injections were done with 10 mM glycine (pH 7).

For immunofluorescence, dejellied eggs in 0.1× MMR were fixed by transferring to 90% methanol and 50 mM ethylene glycol tetraacetic acid. After 24 h of gentle agitation at room temperature, eggs were transferred to 100% methanol and moved to 4°C, where they can be stored for months. To probe with antibodies, eggs were rehydrated through a series of methanol–Tris-buffered saline (TBS; 50 mM Tris, pH 7.5, 150 mM NaCl) mixtures (75, 50, 25% methanol, 15 min each with gentle agitation) and finally transferred to TBS. They were then hemisected and bleached overnight in a hydrogen peroxide (JT Baker, Center Valley, PA)/formamide mixture. Directly labeled antibodies were used at approximately the following concentrations: Alexa 488–tubulin (1–2 µg/ml), Alexa 647–AurB kinase (0.5 µg/ml), and Alexa 568–Kif23 (1–2 µg/ml). See the Methods section in Nguyen, Groen, *et al*. (2014) for full protocol and more information on antibodies. (All Alexa dyes are from Thermo Fisher Scientific, Waltham, MA.)

Light microscopy for fixed eggs

Fixed *Xenopus* eggs were imaged with a laser scanning confocal microscopes at two locations. At the Nikon Imaging Center at Harvard Medical School, a 10× dry and a 20× multi-immersion objective (Nikon, Melville, NY) was used on a Nikon Ti-E inverted microscope with a Nikon A1R point scanning confocal head driven by NIS-Elements image acquisition software. At the Marine Biological Laboratory (Woods Hole, MA), a Zeiss 780 LSM (laser scanning confocal) was used on an inverted Observer Z1 microscope with a motorized stage driven by ZEN software with a 10× dry objective (Zeiss, Thornwood, NJ).

Extract experiments

Actin-intact, cytostatic factor (CSF)–arrested *Xenopus* extract from unfertilized eggs was prepared as described, kept on ice, and used within 8 h (Field *et al*., 2014). Fluorescence probes were prepared and used as described in Nguyen, Groen *et al*. (2014). General methods for imaging microtubules in the egg extract system have been described (Desai *et al*., 1999; Maresca and Heald, 2006).

To initiate microtubule aster growth, extract containing fluorescent probes was converted to interphase by addition of $CaCl_2$ to 0.4 mM, incubated at 20°C for 3 min, and transferred to ice. Calcium addition mimics fertilization and releases CSF arrest (Field *et al*., 2014). Two methods were used to nucleate microtubule asters: either AurkA-coated magnetic beads (Protein A Dynabeads; Thermo Fisher Scientific; Tsai and Zheng, 2005; Nguyen, Groen, *et al*., 2014) or permeabilized *Xenopus* sperm (Murray, 1991) were added. The reaction was spread between two coverslips that had been passivated by coating with polylysine–poly(ethylene glycol) (PEG).

Coverslips were coated with polylysine PEG (PLL(20)-g{3.5}-PEG(2); SuSOS Chemicals, Dubendorf, Switzerland) using a simplified method. Coverslips were dipped in 70% ethanol, flamed, cooled, and placed onto a droplet of 100 µg/ml polylysine-PEG in 100 µM HEPES, pH 7.4, on Parafilm for 15–30 min. They were then washed twice with water for 5 min each and dried with a jet of nitrogen and used the same day.

Reactions were imaged by wide-field fluorescence at 20°C, using a 10× or 20× Plan Apo 1.4 numerical aperture objective lens (Nikon) on an upright Nikon Eclipse 90i microscope equipped with a Prior Lumen 200 metal arc lamp, a Prior ProScan III motorized XY stage (Prior Scientific, Rockland, MA), and a Hamamatsu ORCA-ER cooled charge-coupled camera (Hamamatsu, Japan) and driven by MetaMorph image acquisition software (Molecular Devices, Sunnyvale, CA).

Starting-distance experiments

Interphase asters were nucleated using AurkA beads in extract containing Alexa 488–labeled tubulin and Alexa 647–labeled anti-AurkB IgG. The extract was assembled between PEG-coated coverslips. Two-color time-lapse sequences were taken of multiple image fields in parallel at 1.5- min intervals, starting from ~7–9 min of assembly of the reaction. Bead pairs were identified from the last frame of the tubulin movie (at ~50–55 min), based on whether their asters interacted. For each pair, the initial distance between the beads was measured from the first frame of the AurkB movie (at 9 min). The time of initial contact between each aster within a pair was estimated from the tubulin movie, and an interaction was scored based on the AurkB movie using the following criteria: 1) was CPC recruited to the zone within the next four frames (i.e., 6 min), and 2) was CPC recruited without lateral spreading from a neighboring zone? Zones satisfying both criteria were scored as CPC-positive. Zones not satisfying criterion 1 were scored as CPC-negative, even though they might acquire CPC from lateral spreading at a later time point. Zones satisfying criterion 1 but not criterion 2 (i.e., they acquired CPC via lateral spreading from a neighboring zone) were scored as ambiguous and omitted from further analysis.

Aster with chromatin experiments

Demembranated *Xenopus* sperm labeled with Hoechst (B2261; Sigma-Aldrich) plus labeled tubulin and GFP-DasraA were added to extract and preincubated for 20 min on ice to allow Dasra exchange. Ca^{2+} was added to initiate interphase, and extract was spread between PEG-passivated coverslips. Fields were chosen for imaging based on DNA images alone and were filmed for ~30 min. Asters were scored for the presence of polarized GFP-DasraA at the tips of microtubules on the side of the aster containing the sperm (arcs <50% of the circular aster perimeter). To measure statistics of aster polarization, we quantified 118 asters in 35 fields. Of these, 103 (87%) exhibited polarized recruitment of the Dasra probe to the aster periphery at the 6- or 9-min time point. Polarization was harder to score at later time points because asters tended to interact, and the CPC sometimes spread all around the circumference of the aster. When polarization occurred, the Dasra-positive arc was always on the same side as the chromatin ($n = 103$). Asters growing from free centrosomes ($n = 18$) never recruited GFP-DasraA to microtubule tips unless they were close another aster.

ACKNOWLEDGMENTS

We thank Martin Wuhr for intellectual support and critical reading of the manuscript and Keisuke Ishihara and James Pelletier for critical reading of the manuscript. This work was supported by National Institutes of Health Grant GM39565 (T.J.M.) and MBL fellowships from the Evans Foundation, MBL Associates, and the Colwin Fund (T.J.M. and C.M.F.). We thank the Nikon Imaging Center at Harvard Medical School for microscopy support and the National *Xenopus* Resource at MBL for *Xenopus* animals and care.

REFERENCES

Boldface names denote co–first authors.

Argiros H, Henson L, Holguin C, Foe V, Shuster CB (2012). Centralspindlin and chromosomal passenger complex behavior during normal and Rappaport furrow specification in echinoderm embryos. Cytoskeleton (Hoboken) 69, 840–853.

Baruni JK, Munro EM, von Dassow G (2008). Cytokinetic furrowing in toroidal, binucleat and anucleate cells in C. elegans embryos. J Cell Sci 121, 306–316.

Basant A, Lekomtsev S, Tse YC, Zhang D, Longhini KM, Petronczki M, Glotzer M (2015). Aurora B kinase promotes cytokinesis by inducing centralspindlin oligomers that associate with the plasma membrane. Dev Cell 33, 204–215.

Bieling P, Telley IA, Surrey T (2010). A minimal midzone protein module controls formation and length of antiparallel microtubule overlaps. Cell 142, 420–432.

Brachet PA (1910). La polyspermie expérimentale comme moyen d'analyse de la fécondation. Arch Entwicklungsmechanik Org 30, 261–303.

Canman JC, Cameron LA, Maddox PS, Straight A, Tirnauer JS, Mitchison TJ, Fang G, Kapoor TM, Salmon ED (2003). Determining the position of the cell division plane. Nature 424, 1074–1078.

Carmena M, Wheelock M, Funabiki H, Earnshaw WC (2012). The chromosomal passenger complex (CPC): from easy rider to the godfather of mitosis. Nat Rev Mol Cell Biol 13, 789–803.

Cooke CA, Heck MM, Earnshaw WC (1987). The inner centromere protein (INCENP) antigens: movement from inner centromere to midbody during mitosis. J Cell Biol 105, 2053–2067.

Delacour-Larose M, Molla A, Skoufias DA, Margolis RL, Dimitrov S (2004). Distinct dynamics of Aurora B and Survivin during mitosis. Cell Cycle 3, 1418–1426.

Desai A, Murray A, Mitchison TJ, Walczak CE (1999). The use of *Xenopus* egg extracts to study mitotic spindle assembly and function in vitro. Methods Cell Biol 61, 385–412.

Eggert US, Mitchison TJ, Field CM (2006). Animal cytokinesis: from parts list to mechanisms. Annu Rev Biochem 75, 543–566.

Ferreira JG, Pereira AJ, Akhmanova A, Maiato H (2013). Aurora B spatially regulates EB3 phosphorylation to coordinate daughter cell adhesion with cytokinesis. J Cell Biol 201, 709–724.

Field CM, Nguyen PA, Ishihara K, Groen AC, Mitchison TJ (2014). *Xenopus* egg cytoplasm with intact actin. Methods Enzymol 540, 399–415.

Foe VE, von Dassow G (2008). Stable and dynamic microtubules coordinately shape the myosin activation zone during cytokinetic furrow formation. J Cell Biol 183, 457–470.

Fuller BG, Lampson MA, Foley EA, Rosasco-Nitcher S, Le KV, Tobelmann P, Brautigan DL, Stukenberg PT, Kapoor TM (2008). Midzone activation of aurora B in anaphase produces an intracellular phosphorylation gradient. Nature 453, 1132–1136.

Glotzer M (2005). The molecular requirements for cytokinesis. Science 307, 1735–1739.

Gruneberg U, Neef R, Honda R, Nigg EA, Barr FA (2004). Relocation of Aurora B from centromeres to the central spindle at the metaphase to anaphase transition requires MKlp2. J Cell Biol 166, 167–172.

Herlant M (1911). Recherches sur les oeufs di-et-trispermiques de grenouille. Arch Biol 26, 103–336.

Hu C-K, Coughlin M, Field CM, Mitchison TJ (2008). Cell polarization during monopolar cytokinesis. J Cell Biol 181, 195–202.

Hu C-K, Coughlin M, Field CM, Mitchison TJ (2011). KIF4 regulates midzone length during cytokinesis. Curr Biol 21, 815–824.

Ishihara K, Nguyen PA, Groen AC, Field CM, Mitchison TJ (2014). Microtubule nucleation remote from centrosomes may explain how asters span large cells. Proc Natl Acad Sci USA 111, 17715–17722.

Kelly AE, Sampath SC, Maniar TA, Woo EM, Chait BT, Funabiki H (2007). Chromosomal enrichment and activation of the aurora B pathway are coupled to spatially regulate spindle assembly. Dev Cell 12, 31–43.

Kitagawa M, Fung S Y, Hammeed U F, Goto H, Ingaki M, Lee SH (2014). Cdk1 coordinates timely activation of MKlp2 kinesisn with relocation of the chromosome passenger complex for cytokinesis. Cell Rep 7, 166–179.

Kitagawa M, Lee SH (2015). The chromosomal passenger complex (CPC) as a key orchestrator of orderly mitotic exit and cytokinesis. Front Cell Dev Biol 3, 14.

Lewellyn L, Carvalho A, Desai A, Maddox AS, Oegema K (2011). The chromosomal passenger complex and centralspindlin independently contribute to contractile ring assembly. J Cell Biol 193, 155–169.

Maresca TJ, Heald R (2006). Methods for studying spindle assembly and chromosome condensation in *Xenopus* egg extracts. Methods Mol Biol 322, 459–474.

Mitchison TJ, Nguyen P, Coughlin M, Groen AC (2013). Self-organization of stabilized microtubules by both spindle and midzone mechanisms in *Xenopus* egg cytosol. Mol Biol Cell 24, 1559–1573.

Mitchison T, Wühr M, Nguyen P, Ishihara K, Groen A, Field CM (2012). Growth, interaction, and positioning of microtubule asters in extremely large vertebrate embryo cells. Cytoskeleton (Hoboken) 69, 738–750.

Murati-Hori M, Wang Y-L (2002). Both midzone and astral microtubules are involved in the delivery of cytokinesis signals: insights from the mobility of Aurora B. J Cell Biol 159, 45–53.

Murray AW (1991). Cell cycle extracts. Methods Cell Biol 36, 581–605.

Nguyen PA, Groen AC, Loose M, Ishihara K, Wühr M, Field CM, Mitchison TJ (2014). Spatial organization of cytokinesis signaling reconstituted in a cell-free system. Science 346, 244–247.

Nunes Bastos R, Gandhi SR, Baron RD, Gruneberg U, Nigg EA, Barr FA (2013). Aurora B suppresses microtubule dynamics and limits central spindle size by locally activating KIF4A. J Cell Biol 202, 605–621.

Ohi R, Sapra T, Howard J, Mitchison TJ (2004). Differentiation of cytoplasmic and meiotic spindle assembly MCAK functions by Aurora B-dependent phosphorylation. Mol Biol Cell 15, 2895–2906.

Rappaport R (1961). Experiments concerning the cleavage stimulus in sand dollar eggs. J Exp Zool 148, 81–89.

Rappaport R (1969). Aster-equatorial surface relations and furrow establishment. J Exp Zool 171, 59–68.

Rappaport R (2005). Cytokinesis in Animal Cells, Cambridge, UK: Cambridge University Press.

Render JA, Elinson RP (1986). Axis determination in polyspermic *Xenopus* laevis eggs. Dev Biol 115, 425–433.

Rieder CL, Khodjakov A, Paliulis LV, Fortier TM, Cole RW, Sluder G (1997). Mitosis in vertebrate cells with two spindles: implications for the anaphase onset checkpoint and cleavage. Proc Natl Acad Sci USA 94, 5107–5112.

Savoian MS, Earnshaw WC, Khojakov A, Rieder CL (1999). Cleavage furrows formed between centrosome lacking an intervening spindle and chromosome contain microtuble bundles, INCENP, and CHO1 but not CENP-E. Mol Biol Cell 10, 297–311.

Sive H, Grainger R, Harland R (2000). Early Development of *Xenopus* Laevis: A Laboratory Manual, Cold Spring Harbor, NY: Cold Spring Harbor Laboratory Press.

Snook RR, Hosken DJ, Karr TL (2011). The biology and evolution of polyspermy: insights from cellular and functional studies of sperm and centrosomal behavior in the fertilized egg. Reproduction 142, 779–792.

Tsai M-Y, Zheng Y (2005). Aurora A kinase-coated beads function as microtubule-organizing centers and enhance RanGTP-induced spindle assembly. Curr Biol 15, 2156–2163.

Tseng BS, Tan L, Kapoor TM, Funabiki H (2010). Dual detection of chromosomes and microtubules by the chromosomal passenger complex drives spindle assembly. Dev Cell 18, 903–912.

Tsuchiya Y, Murai S, Yamashita S (2005). Apoptosis-inhibiting activities of BIR family proteins in *Xenopus* egg extracts. FEBS J 272, 2237–2250.

Walczak CE, Mitchison TJ, Desai A (1996). XKCM1: a *Xenopus* kinesin-related protein that regulates microtubule dynamics during mitotic spindle assembly. Cell 84, 37–47.

White EA, Glotzer M (2012). Centralspindlin: at the heart of cytokinesis. Cytoskeleton (Hoboken) 69, 882–892.

Wühr M, Dumont S, Groen AC, Needleman DJ, Mitchison TJ (2009). How does a millimeter-sized cell find its center? Cell Cycle 8, 1115–1121.

Wühr M, Freeman RM, Presler M, Horb ME, Peshkin L, Gygi SP, Kirschner MW (2014). Deep proteomics of the *Xenopus* laevis egg using an mRNA-derived reference database. Curr Biol 24, 1467–1475.

Zimniak T, Stengl K, Mechtler K, Westermann S (2009). Phosphoregulation of the budding yeast EB1 homologue Bim1p by Aurora/Ipl1p. J Cell Biol 186, 379–391.